Molecular Biology of the Cell
Vol. 17, 2869–2881, July 2006

PAK1 and aPKCζ Regulate Myosin II-B Phosphorylation: A Novel Signaling Pathway Regulating Filament Assembly

Liron Even-Faitelson and Shoshana Ravid

Department of Biochemistry, Institute of Medical Sciences, Faculty of Medicine, The Hebrew University, Jerusalem 91120, Israel

Submitted November 2, 2005; Revised March 28, 2006; Accepted April 5, 2006
Monitoring Editor: Martin A. Schwartz

Many signaling pathways regulate the function of the cellular cytoskeleton. Yet we know very little about the proteins involved in the cross-talk between the signaling and the cytoskeletal systems. Here we show that myosin II-B, an important cytoskeletal protein, resides in a complex with p21-activated kinase 1 (PAK1) and atypical protein kinase C (PKC) zeta (aPKCζ) and that the interaction between these proteins is EGF-dependent. We further show that PAK1 is involved in aPKCζ phosphorylation and that aPKCζ phosphorylates myosin II-B directly on a specific serine residue in an EGF-dependent manner. This latter phosphorylation is specific to isoform B of myosin II, and it leads to slower filament assembly of myosin II-B. Furthermore, a decrease in aPKCζ expression in the cells alters myosin II-B cellular organization. Our finding of a new signaling pathway involving PAK1, aPKCζ, and myosin II-B, which is implicated in myosin II-B filament assembly and cellular organization, provides an important link between the signaling system and cytoskeletal dynamics.

INTRODUCTION

The cytoskeleton consists of a complex network of proteins responsible for many cellular processes such as adhesion, cytokinesis, and cell motility. To be able to perform these functions the cytoskeleton must be highly dynamic and reorganize rapidly in specific regions of the cell in response to extracellular signals. Nonmuscle myosin II is an important part of this complex cytoskeletal network and plays a major role in its functions.

Myosin II is a hexamer composed of two heavy chains of 200 kDa and two pairs of light chains (MLCs). Whereas the regulation of MLC has been extensively investigated, little is known about the regulation and phosphorylation of the myosin heavy chains. In vertebrates, there are at least three nonmuscle myosin II heavy chain (NMHC) genes that encode separate isoforms of the heavy chain: NMHC II-A, NMHC II-B, and NMHC II-C (Katsuragawa *et al.,* 1989; Kawamoto and Adelstein, 1991; Berg *et al.,* 2001; Buxton *et al.,* 2003). These isoforms have different tissue and cellular distribution and different functions (Cheng *et al.,* 1992; Miller *et al.,* 1992; Maupin *et al.,* 1994; Rochlin *et al.,* 1995; Kelley *et al.,* 1996; Straussman *et al.,* 2001).

Nonmuscle myosin II needs to undergo dynamic assembly–disassembly for it to function within a cell. Murakami *et al.* have shown that the filament assembly–disassembly of myosin II-A and myosin II-B are separately regulated. The filament assembly of myosin II-A is regulated mainly by the binding of the protein Mts1, although recent work has show that it is also regulated by phosphorylation (Dulyaninova *et al.,* 2005), whereas myosin II-B assembly is regulated by phosphorylation of the nonhelical C-terminal domain of NMHC II-B (Murakami *et al.,* 1998, 2000). We have recently shown that NMHC II-B phosphorylation in response to EGF is necessary for its localization within the cell and that NMHC II-B plays a crucial role in chemotaxis (Straussman *et al.,* 2001; Ben-Ya'acov and Ravid, 2003).

Mammalian p21-activated kinases (PAKs) have been implicated in the regulation of a number of cellular activities, including regulation of MAP kinase signaling pathways, apoptosis and the cell cycle, and cytoskeletal dynamics (Knaus and Bokoch, 1998). PAKs are effector proteins of the Rho small GTPases, Rac and Cdc-42, and this family of serine/threonine kinases comprises six members (Jaffer and Chernoff, 2002). Recently, van Leeuwen *et al.* (1999) have shown that PAK1 is involved in the bradykinin-dependent phosphorylation of NMHC in PC12 cells. Moreover, we have recently shown that PAK1 is involved in the regulation of myosin II-B phosphorylation, localization, and filament assembly (Even-Faitelson *et al.,* 2005).

Another family of serine/threonine kinases, the PKCs, play a central role in many signal transduction pathways in the cell. The PKC family is divided into three main groups with different structures and different activators. The conventional PKCs, including cPKCα, cPKCβI, cPKCβII, and cPKCγ, require phosphatidylserine (PS), Ca^{2+}, and diacylglycerol (DAG) to activate them. Novel PKCs, including nPKCδ, nPKCε, nPKCη, and nPKCθ, require only PS and DAG. Finally, atypical PKCs, such as aPKCλ, aPKCι, and aPKCζ, require only PS to activate them.

Among playing a role in many cell signaling pathways, PKC appears to be an important regulator in cytoskeletal function. It has been shown that PKC and cytoskeletal proteins are colocalized, treatment of cells with PKC activators causes cytoskeletal rearrangement, and PKC phosphorylates cytoskeletal proteins (Keenan and Kelleher, 1998). Various

This article was published online ahead of print in *MBC in Press* (http://www.molbiolcell.org/cgi/doi/10.1091/mbc.E05–11–1001) on April 12, 2006.

Address correspondence to: Shoshana Ravid (ravid@cc.huji.ac.il).

Abbreviations used: PAK1, p21-activated kinase 1; aPKCζ, atypical PKC zeta; MLC, myosin light chain; NMHC, non-muscle myosin II heavy chain; IP-PAK1, immunoprecipitated PAK1; CKII, casein kinase II.

studies show that PKC is involved in regulating MLC either directly or by regulating MLC-kinase (Ikebe *et al.*, 1985, 1987; Turbedsky *et al.*, 1997). PKC also appears to play a role in the regulation of NMHC (Murakami *et al.*, 1998; Straussman *et al.*, 2001; Su and Kiehart, 2001). Furthermore, aPKCζ is involved in actin cytoskeletal regulation (Gomez *et al.*, 1995, 1997; Laudanna *et al.*, 1998; Uberall *et al.*, 1999; Hellbert *et al.*, 2000; Chodniewicz and Zhelev, 2003). Uberall *et al.* (1999) have suggested that aPKCζ works downstream to Rac1 in Ras-mediated rearrangement of the actin cytoskeleton. Additionally, Laudanna *et al.* (1998) have shown that aPKCζ is involved in the signaling pathway, leading to chemoattractant-triggered actin assembly, integrin-dependent adhesion, and chemotaxis of polymorphonuclear neutrophils.

The many important cellular functions of the cytoskeleton have generated intensive investigation of cellular signaling pathways influencing the cytoskeletal meshwork. Here we provide evidence for a novel signal transduction pathway that begins with the stimulation of TSU-pr1 cells with EGF and ends with the phosphorylation of NMHC II-B by aPKCζ, which functions downstream to PAK1. This signaling pathway is involved in the regulation of myosin II-B filament assembly and cellular organization.

MATERIALS AND METHODS

Cell Line and Culture Conditions

The cell line used here was a prostate carcinoma cell line, TSU-pr1 (Iizumi *et al.*, 1987). This cell line was derived from human prostate adenocarcinoma, metastatic to lymph node (kindly provided by Dr. Antonnino Passaniti, University of Maryland National Institute of Health, Baltimore, MD). Cells were maintained as described previously (Ben-Ya'acov and Ravid, 2003). COS-7 and HEK-293 cell lines were maintained as described previously (Rosenberg and Ravid, 2006).

Antibodies and Reagents

The following antibodies were used in this work: PAK1 (N-20), aPKCζ, cPKCβII, Cdk7 antibodies (Santa Cruz Biotechnology, Santa Cruz, CA), HA antibodies (Roche, Basel, Switzerland), affinity-purified specific polyclonal antibodies against the C-terminal of NMHC II-B (Straussman *et al.*, 2001; Ben-Ya'acov and Ravid, 2003) or against GFP, cPKCγ, nPKCε, and aPKCι antibodies (BD Transduction Laboratories, San Jose, CA), and PAK1 and p42-MAP Kinase (p42-MAPK) antibodies (Cell Signaling Technology, Danvers, MA). All other reagents, unless otherwise specified, were purchased from Sigma (St. Louis, MO).

Immunoprecipitation of PAK1 from TSU-pr1 Cells and In Vitro Phosphorylation

Immunoprecipitation of PAK1 from TSU-pr1 cells was carried out as described previously (Even-Faitelson *et al.*, 2005). The IP-PAK1 was used to phosphorylate 10 μg MBP, NMHC II-A, or NMHC II-B in an in vitro activity assay described previously (Even-Faitelson *et al.*, 2005). The samples were separated on SDS-PAGE, and the extent of phosphorylation was measured by counting the bands in a scintillation counter. The relative phosphorylation was calculated by dividing the phosphorylation level of each protein by the phosphorylation level of that same protein without EGF stimulation.

Coimmunoprecipitation, Gel Electrophoresis, and Western Blotting

Cells, 5×10^5, were starved to serum as described previously (Even-Faitelson *et al.*, 2005) and then stimulated with 7 ng ml^{-1} EGF for 0, 1, or 4 min. At the indicated time points, the plated cells were washed with ice-cold phosphate-buffered saline (PBS) and then collected in 300 μl sonication buffer (50 mM Tris-HCl, pH 7.5, 50 mM NaCl, 1 mM DTT, 2 mM EDTA, Protease Inhibitors Cocktail). Cells were then sonicated, incubated for 15 min on ice, and centrifuged at 25,000 × *g* for 15 min at 4°C. Supernatants were transferred to fresh tubes and rotated at 4°C for 2 h with protein A/G agarose beads (Pierce, Rockford, IL) coupled covalently to polyclonal PAK1 antibodies, affinity-purified specific polyclonal antibodies against the C-terminal of NMHC II-B, monoclonal aPKCζ antibodies, polyclonal Cdk7 antibodies, or beads only. Cdk7 antibodies or beads only were used as negative control for the coimmunoprecipitation experiments. The covalent coupling was performed essentially as described (Simanis and Lane, 1985). Briefly, the beads were washed twice with 0.2 M sodium borate, pH 9.0, incubated o/n at RT with 20 mM dimethyl pimelimidate dihydrochloride and then washed twice and incubated for 2 h at RT with 0.2 M ethanolamine, pH 8.0. The beads–antibody complex was then washed three times with sonication buffer and resuspended in SDS-PAGE sample buffer. For the coimmunoprecipitation of PAK1 with NMHC II-B and aPKCζ the cells were transiently transfected with pCMV6M-PAK1 (kindly provided by Dr. Gary M. Bokoch, The Scripps Research Institute), and the rest of the procedure was carried out as described above. Whole cell extract were prepared by lysing the same amount of cells used for immunoprecipitation with SDS-PAGE sample buffer. Only half of the amount of the total whole cell extract was loaded on each gel. Samples were separated on 10% SDS-PAGE, and Western blotting was performed using standard procedures using the same antibodies used for the immunoprecipitation and cPKCβII, cPKCγ, nPKCε, and aPKCι antibodies.

NMHC II-A and NMHC II-B Tail Phosphorylation by Recombinant aPKCζ or GST-PAK1

Phosphorylation of NMHC II-A and NMHC II-B tails using recombinant aPKCζ (Sigma) was performed according to the manufacturer's instructions. Briefly, 10 μg of NMHC II-A or NMHC II-B tail in "tail mix" (25 mM Tris-HCl, pH 7.5, 5 mM $MgCl_2$, 0.5 mM EGTA, 1 mM DTT, 100 μM ^{32}P-γATP [Amersham Pharmacia Biotech, Piscataway, NJ], and 10 μl/sample Lipid mix [prepared according to manufacturer's instructions]) were either mixed with diluted recombinant aPKCζ, dilution buffer (as specified by the manufacturer) without the enzyme or with TSU-pr1 cell lysate and incubated at 30°C for 20 min. The reaction was stopped by the addition of cold 10% TCA. Samples were washed with 5% TCA, resuspended in SDS-PAGE sample buffer, and separated on 12% SDS-PAGE. Gels were stained and phosphorylation of NMHC II-A and NMHC II-B tails was determined by exposing the gels to film or by cutting the bands and counting them in a scintillation counter. To achieve the best enzyme-substrate ratio for maximum phosphorylation of NMHC II-B tail by aPKCζ, several quantities of substrate (0.01, 0.1, 0.5 μg) and enzyme (0.02, 0.05, 0.08 μg) were used. Phosphate incorporation (mol phosphate per mol NMHC II-B tail) was calculated according to the following formula: (cpm × nmol ATP in the reaction/total cpm)/nmol NMHC II-B tail in the reaction.

NMHC II-B tail or MBP phosphorylation by PAK1 was performed using GST-PAK1 (kindly provided by Dr. Gary M. Bokoch, The Scripps Research Institute). GST-PAK1, 1 μg, was used to phosphorylate 1 μg substrate (NMHC II-B tail or MBP) in PAK1 kinase buffer (50 mM HEPES, pH 7.5, 10 mM $MgCl_2$, 2 mM $MnCl_2$, 0.2 mM DTT). The reaction was initiated by the addition of 20 μM ATP and 0.5 μCi ^{32}P-γATP. The reaction was stopped by the addition of 15 μl 5× SDS-PAGE sample buffer. Phosphorylation levels were determined as described above.

Expression, Immunoprecipitation, and Phosphorylation of GFP-NMHC II-B by aPKCζ

pEGFP-C3-NMHC II-B full length (kindly provided by Dr. R. S. Adelstein, Laboratory of Molecular Cardiology, NIH) was transfected to ~60% confluent COS-7 cells on 60-mm plates using jetPEI transfection reagent (Polyplus-transfection, Strasbourg, France). Forty-eight hours after the transfection the cells were washed once with cold PBS and lysed with 400 μl modified lysis buffer for activity assay (50 mM Tris-HCl, pH 7.5, 5 mM EDTA, 150 mM NaCl, 50 mM NaPPi, 100 mM NaF, 0.2% Triton X-100). The GFP-NMHC II-B was immunoprecipitated as described above using affinity-purified rabbit polyclonal GFP antibodies. The immunoprecipitates were washed twice with the modified lysis buffer for activity assay, twice with lysis buffer for activity assay (50 mM Tris-HCl, pH 7.5, 5 mM EDTA, 50 mM NaCl, 0.2% Triton X-100), and once with washing buffer (25 mM Tris-HCl, pH 7.5, 5 mM $MgCl_2$, 0.5 mM EGTA). The phosphorylation reaction was carried out using recombinant aPKCζ, essentially as described above. The samples were separated on 6% SDS-PAGE, stained with Coomassie brilliant blue, scanned, dried, and exposed to film.

aPKCζ Phosphorylation by Recombinant GST-PAK1

pCDNA3-HA-aPKCζ$^{WT/KD(K281R)}$ (kindly provided by Dr. Yehiel Zick, The Weizmann Institute) or pEGFP (Clontech, San Jose, CA) control were transfected to HEK-293 cells using the calcium-phosphate transfection protocol (Chen and Okayama, 1987). After 24 h the cells were lysed with Buffer H (50 mM β-glycerophosphate, pH 7.4, 1.5 mM EGTA, 1 mM EDTA, 1 mM DTT, 50 mM NaCl, 0.1 mM Na_3VO_4, 0.5% NP-40, Protease Inhibitor Cocktail), incubated on ice, and centrifuged as described above. The supernatants were incubated with Ultralink Immobilized Protein G (Pierce) bound to anti-HA antibodies for 2 h at 4°C. To remove any protein that may have coimmunoprecipitated with aPKCζ, the complex was washed stringently: twice with 1% NP-40 in PBS, twice with 10 mM Tris, pH 7.5, 0.5 M LiCl; once with 10 mM Tris, pH 7.5, 100 mM NaCl, 1 mM EDTA; and twice with PAK1 kinase buffer described above. Kinase assay was performed on the immunoprecipitates as described above for the phosphorylation of MBP/NMHC II-B tail by GST-PAK1.

In Vivo Phosphorylation of TailB-6A and TailB-7A

A 530-base pair C-terminal fragment of NMHC II-B in which 7 serine residues were mutated to alanine residues (amino acids 1922, 1935, 1937, 1938, 1939, 1941, and 1952, see Figure 6A) was restricted from pET21C vector (Novagen, San Diego, CA) using XhoI and SmaI (Fermentas, Ontario, Canada) and cloned into pEGFP-C3 (Clontech) using the same restriction sites (pEGFP-TailB7A). A site-directed mutagenesis reaction (QuikChange, Stratagene, La Jolla, CA) was carried out on the above pEGFP-TailB7A to convert back the alanine at position 1937 to serine (pEGFP-TailB6A). The mutations were verified by DNA sequencing (Center for Genomic Analysis, The Hebrew University, Jerusalem, Israel).

TSU-pr1 cells, 8×10^5, were seeded on 60-mm plates, and pEGFP-TailB-6A or pEGFP-TailB-7A were transfected to the cells using jetPEI (Polyplus-transfection) ~44 h before the experiment. Cells were washed twice in 2 ml prewarmed RPMI-H (Even-Faitelson *et al.*, 2005) without phosphate and then incubated for 2 h with 3 ml RPMI-H containing 80 μCi ^{32}P orthophosphate (Amersham Pharmacia Biotech). After 2 h half the plates were treated with 10 μM cell permeable aPKCζ inhibitor (myristoylated pseudosubstrate, Biosource, Camarillo, CA) for 50 min (Etienne-Manneville and Hall, 2003). Next, the plates were either not stimulated or stimulated for 1 min with EGF and then washed with PBS and lysed with 1× RIPA (50 mM Tris-HCl, pH 7.5, 1% NP-40, 0.5% deoxycholic acid, 50 mM sodium pyrophosphate, 100 mM sodium fluoride, and protease inhibitor mix). Lysates were incubated on ice and centrifuged as described above, and the supernatants were incubated overnight with protein A-agarose (Pierce) that were preincubated and cross-linked to NMHC II-B antibodies described above. After incubation, the complex was washed three times with 1× RIPA and loaded on 10% SDS-PAGE. The gels were stained with Coomassie, scanned, dried, and exposed to an autoradiogram. The amount of the proteins and their phosphorylation levels were quantified using Fujifilm ImageGauge Ver. 3.4 (Fuji, Tokyo, Japan). To standardize the phosphorylation level to protein quantity, the value of phosphorylation was divided by the total protein value. Then, the percent of phosphorylated protein after treatment with the inhibitor was calculated by dividing the standardized phosphorylation of the inhibitor treated sample by the standardized phosphorylation of the untreated sample at the same time point. To calculate the relative phosphorylation of EGF-stimulated Tail-6A compared with unstimulated Tail-6A, the standardized phosphorylation of the EGF-stimulated sample in each experiment was divided by the value of the standardized phosphorylation of the unstimulated sample in the same experiment. The average relative phosphorylation was calculated from the results of three separate experiments.

siRNA of PAK1 or aPKCζ and In Vivo Phosphorylation of aPKCζ or NMHC II-B, Respectively

siRNA of PAK1 was carried out using *SignalSilence* PAK1 siRNA (Cell Signaling Technology). For a control, *SignalSilence* nonspecific fluorescein-conjugated siRNA was used (Cell Signaling Technology). siRNA of aPKCζ was carried out using Dharmacon's *SMART*pool siRNA designated to target aPKCζ (Dharmacon, Lafayette, CO). As a control, si*CONTROL* NonTargeting siRNA Pool was used (Dharmacon). Transfection of the siRNA to the cells was carried out using *Trans*IT-TKO transfection reagent according to the manufacturer's instructions (Mirus, Madison, WI). Briefly, TSU-pr1 cells were seeded on 60-mm plates to reach ~70% confluence on the day of transfection and then transfected with 100 nM PAK1 siRNA, 50 nM aPKCζ *SMART*pool siRNA, or 25 nM control siRNA. Cells were incubated for 48 h before performing the experiment. To monitor transfection efficiency, on the day of the experiment the control siRNA cells were observed using a fluorescence microscope.

The in vivo phosphorylation assay was carried out essentially as described above for the phosphorylation of TailB-6A and TailB-7A, but with a few modifications. The siRNA-treated cells were washed and incubated with RPMI-H (Even-Faitelson *et al.*, 2005) without phosphate containing 80 μCi ^{32}P orthophosphate and then incubated as described above. The EGF-stimulated and unstimulated cells were then lysed, as described above. Ten percent of the cleared lysate was used for testing PAK1 or aPKCζ siRNA efficiency using Western blot analysis, and the rest of the lysate was used for immunoprecipitation of aPKCζ or NMHC II-B. The immunoprecipitates and lysates were separated on 10% SDS-PAGE, or 6% for NMHC II-B. The lysates were transferred to nitrocellulose membrane and Western blotting was performed as described above using PAK1 antibodies (Santa Cruz or Cell Signaling Technology) and p42-MAPK antibodies (Cell Signaling Technology) for loading control, or aPKCζ antibodies (Santa Cruz) and p42-MAPK antibodies. The gel with the aPKCζ immunoprecipitates was silver-stained using silverSNAP kit (Pierce) and then scanned, dried, and exposed to film. The gel with the NMHC II-B immunoprecipitates was stained using Coomassie brilliant blue, scanned, dried, and exposed to film. The quantification was carried out as described above. The decrease in PAK1 or aPKCζ expression was calculated by dividing the amount of PAK1 or aPKCζ with the amount of p42-MAPK and comparing between the lysates from cells that were transfected with PAK1 siRNA or aPKCζ *SMART*pool siRNA and lysates from cells that were transfected with control siRNA. Standardization of the phosphorylation level of aPKCζ or NMHC II-B to the total aPKCζ or NMHC II-B immunoprecipitated was done as described above. In each experiment the phosphorylation level of aPKCζ or NMHC II-B of each sample was divided by the value of phosphorylated aPKCζ or NMHC II-B in the control siRNA sample, thus leading to a relative phosphorylation value.

Protein Purification, Critical Concentration, and Solubility Assay

Expression and purification of myosin proteins was carried out essentially as described by (McNally *et al.*, 1991) with a few modifications. Briefly, *Escherichia coli* strain BL-21 containing the pET21c-NMHC II-B rod plasmid, which encodes for 630 amino acids derived from the C-terminal of NMHC II-B (hereafter referred to as NMHC II-B rod), wild-type, or S1937D mutant, were grown to OD_{600} = ~0.6 and then induced with 0.5 mM IPTG for 2 h. Bacteria pellets were lysed with lysis buffer (50 mM Tris-HCl, pH-7.5, 0.8 M NaCl, 10 mM EDTA, 10 mM EGTA, 1 mM DTT, 1 mg/ml lysozyme, and 0.5 mM phenylmethylsulfonyl fluoride) and sonicated. Sonicates were centrifuged, and the DNA was precipitated from the supernatant with 10% polyethylenimine (Burgess, 1991), centrifuged again, and then boiled to denature all proteins except for the α-helical coiled NMHC II-B rod. The mixture was then centrifuged at 100,000 × *g*, and the NMHC II-B rod was precipitated from the supernatant using ammonium sulfate. The ammonium sulfate pellet was solubilized in Buffer G (20 mM Tris-HCl, pH 7.5, 600 mM NaCl, 5 mM EDTA, and 1 mM DTT).

To determine the critical concentration, the proteins were diluted to 15, 25, 50, 100, or 250 μg/ml in Buffer G (20 mM Tris-HCl, pH 7.5, 600 mM NaCl, 5 mM EDTA, and 1 mM DTT). Eighty microliters of each protein concentration were dialyzed for 4 h in 150 mM dialysis buffer (10 mM phosphate buffer, 2 mM $MgCl_2$, and 150 mM NaCl), centrifuged in a TL-100 ultracentrifuge (Beckman Coulter, Fullerton, CA) at 100,000 × *g*, for 1 h at 4°C, and the supernatant and pellet were separated. Twenty microliters of the supernatant and the pellet that was solubilized in 80 μl Buffer G were loaded on 10% SDS-PAGE. The gels were stained with Coomassie brilliant blue, scanned, and quantified using Fujifilm image analyzer LAS-1000plus and the densitometry program Fujifilm ImageGauge Ver. 3.4.

Solubility assays were performed similarly. The proteins were diluted in Buffer G to a concentration of 0.5 mg/ml and dialyzed in 150 mM dialysis buffer. An 80-μl sample was taken at 1, 1.5, 2, 3, and 4 h after the beginning of the dialysis and centrifuged as described above. Forty microliters of the supernatant were diluted in 360 μl Buffer G, and the pellet was solubilized in 800 μl Buffer G. The remaining procedure was as described above.

Microscopy

Indirect immunofluorescent staining was performed as described (Ben-Ya'acov and Ravid, 2003). Cells were stimulated with 7 ng ml^{-1} of EGF for 0, 1, or 4 min at RT. Cells were fixed, permeabilized, and stained using polyclonal antibody specific for the N-terminal domain of NMHC II-B (kindly provided by R. S. Adelstein) and monoclonal antibody for aPKCζ. Immunofluorescence was achieved using goat anti-rabbit IgG conjugated to Cy5 (Jackson ImmunoResearch, West Grove, PA) and goat anti-mouse Alexa 448 (Invitrogen-Molecular Probes, Carlsbad, CA) as secondary antibodies. To quantify the number of cells that show colocalization at each time point of EGF stimulation, several random fields of cells were counted in three individual experiments (average number of cells counted at each time point: n = 180). The cells were classified as showing colocalization or not showing colocalization and the results are presented as the percentage of cells showing colocalization out of the total number of cells counted. For indirect immunofluorescent staining of cells treated with aPKCζ or control siRNA, 48 h after transfection with the siRNA the above procedure was performed. Quantification of cells that show cortical localization of NMHC II-B after EGF stimulation was performed by counting an average of 200 cells, transfected either with aPKCζ siRNA or control siRNA, from 10 random fields.

Mass Spectrometry

NMHC II-B tail, 5 μg, was phosphorylated using 2.5 μg recombinant aPKCζ, as described above, except for the ATP concentration in the mixture, which was 250 μM instead of 100 μM, and ^{32}P-γATP was not present. The sample was separated on 12% SDS-PAGE together with nonphosphorylated NMHC II-B tail, for comparison, and stained with Coomassie brilliant blue. The phosphorylated and unphosphorylated NMHC II-B tail bands were excised from the gel, reduced, alkylated, and digested in-gel using sequencing-grade trypsin (Promega, Madison, WI) as described elsewhere (Pandey *et al.*, 2000). Desalting of the peptide mixture was performed using ZipTip C_{18} column (Millipore, Billerica, MA), and the peptides were eluted using 80% acetonitrile, 1% formic acid. The eluted peptides were directly injected by spraying capillaries (Protana, Toronto, Canada) to a Q-TOF II mass spectrometer (Micromass, Toronto, Canada) equipped with a nanoelectrospray source. MS and MS/MS spectra were measured using 1200 V capillary voltage, and the MS/MS collision energy was 20–45 V.

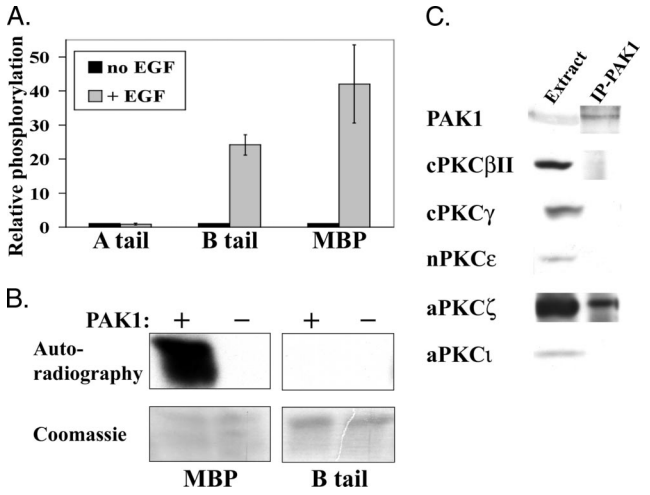

Figure 1. PAK1 is involved in NMHC II-B phosphorylation, but does not phosphorylate it directly. (A) IP-PAK1 phosphorylates NMHC II-B and MBP, but not NMHC II-A, in an EGF-dependent manner. Unstimulated TSU-pr1 cells or cells stimulated with EGF for 1 min were lysed, and PAK1 was immunoprecipitated and used in an in vitro activity assay with NMHC II-A tail, NMHC II-B tail, or MBP as substrates. The samples were separated on SDS-PAGE, and bands were excised and counted in scintillation counter. Results are shown as mean ± SD of three separate experiments. (B) Recombinant GST-PAK1 does not phosphorylate NMHC II-B directly. GST-PAK1 was used in an in vitro activity assay with MBP and NMHC II-B as substrates. The samples were separated on SDS-PAGE, stained with Coomassie, and exposed to autoradiography. The results are representative of three experiments. (C) aPKCζ coimmunoprecipitates with PAK1. The expression of the different PKC isoforms in TSU-pr1 cells was determined by resolving cell extracts on SDS-PAGE followed by Western blot analysis with antibodies specific for the different PKC isoforms. The association between PAK1 and PKC isoforms was determined by immunoprecipitating PAK1 from TSU-pr1 lysates and subjecting it to Western blot analysis with the appropriate antibodies. See *Materials and Methods* for details for this and all other figures.

RESULTS

PAK1 Is Involved in NMHC II-B Phosphorylation, But Does Not Phosphorylate It Directly

We have recently shown that PAK1 is involved in EGF-dependent phosphorylation of NMHC II-B but not in NMHC II-A phosphorylation (Even-Faitelson *et al.,* 2005). Figure 1A shows that stimulation of cells with EGF leads to increased phosphorylation activity of immunoprecipitated PAK1 (IP-PAK1) on NMHC II-B C-terminal fragment (NMHC II-B tail) and on myelin basic protein (MBP) positive control in comparison to IP-PAK1 from unstimulated cells. On the other hand, IP-PAK1 did not show increased phosphorylation on NMHC II-A C-terminal fragment (NMHC II-A tail) in response to EGF stimulation.

Having seen the EGF-dependent phosphorylation activity of IP-PAK1 on NMHC II-B, we next investigated whether PAK1 phosphorylates NMHC II-B directly or serves as an intermediate in the signaling cascade leading to NMHC II-B phosphorylation. To address this query, we used recombinant GST-PAK1 to phosphorylate NMHC II-B tail in an in vitro phosphorylation assay. As shown in Figure 1B, the recombinant GST-PAK1 is active and is able to phosphorylate MBP positive control, but is unable to phosphorylate NMHC II-B directly. Thus far we have shown that PAK1 is involved in NMHC II-B and not NMHC II-A EGF-dependent phosphorylation and that PAK1 does not phosphorylate NMHC II-B directly. It is therefore likely that IP-PAK1 includes a complex of proteins that one of them, other than PAK1, is responsible for the direct phosphorylation of NMHC II-B.

aPKCζ Is Present in the IP-PAK1 Complex That Phosphorylates NMHC II-B

The next step was to search for the protein(s) that interact with PAK1 and are responsible for the direct phosphorylation of NMHC II-B in response to EGF stimulation. Previous studies by us and by other groups confirmed that PKC is involved in NMHC phosphorylation (Conti *et al.,* 1991; Murakami *et al.,* 1994; Murakami *et al.,* 1995, 2000; Straussman *et al.,* 2001; Su and Kiehart, 2001), and we found that TSU-pr1 cells express the PKC isoforms: cPKCβII, cPKCγ, nPKCε, and aPKCζ (Straussman *et al.,* 2001). We therefore investigated which of these PKCs coimmunoprecipitate with PAK1.

We immunoprecipitated PAK1 from TSU-pr1 cell lysates and subjected it to Western blot analysis using specific antibodies against the PKC isoforms. The same amount of cells was used for each immunoprecipitation and, as shown in Figure 1C, only aPKCζ coimmunoprecipitated with PAK1. We went on to examine the involvement of aPKCζ in the regulation of NMHC II-B.

PAK1, aPKCζ, and NMHC II-B Are All Found in One Complex In Vivo

The next step was to show a direct link between PAK1, aPKCζ, and NMHC II-B. To determine whether PAK1, aPKCζ, and NMHC II-B interact in vivo, we immunoprecipitated each of these proteins and checked if they coimmunoprecipitated with each other by subjecting them to Western blot analysis as described in *Materials and Methods.* As shown in Figure 2A, immunoprecipitated NMHC II-B subjected to Western blot analysis with aPKCζ-specific antibody clearly indicates that aPKCζ coimmunoprecipitates with NMHC II-B. Moreover, aPKCζ and PAK1 were immunoprecipitated and subjected to Western blot analysis using NMHC II-B–specific antibody and indeed, as shown in Figure 2A, NMHC II-B coimmunoprecipitated with both aPKCζ and PAK1. Furthermore, in order to see that the interactions are specific, we performed the reciprocal experiment. Figure 2A clearly shows that PAK1 coimmunoprecipitates with both NMHC II-B and aPKCζ. The interactions between aPKCζ, NMHC II-B, and PAK1 are specific because they barely immunoprecipitated with the negative controls. Together these results strongly indicate that PAK1, aPKCζ, and NMHC II-B all reside in one complex in vivo.

As mentioned above, IP-PAK1 phosphorylates NMHC II-B in an EGF-dependent manner. To determine whether the aPKCζ-NMHC II-B interaction is also EGF-dependent, we stimulated TSU-pr1 cells for different time intervals with EGF, immunoprecipitated aPKCζ, and subjected it to Western blot analysis using NMHC II-B specific antibodies (Figure 2B). NMHC II-B coimmunoprecipitated with aPKCζ in an EGF-dependent manner, with a peak of association between NMHC II-B and aPKCζ 1 min after EGF stimulation. The amount of NMHC II-B interacting with aPKCζ decreased 4 min after EGF stimulation, whereas the amount of immunoprecipitated aPKCζ barely changed, as seen in the left panel of Figure 3B. Quantification of several such experiments indicates that there is an increase of ~2.4-fold in the amount of NMHC II-B that coimmunoprecipitates with aPKCζ 1 min after EGF stimulation of cells compared with unstimulated cells (Figure 2C). These results indicate that the interaction between NMHC II-B and aPKCζ is dynamic and EGF-dependent. The coimmunoprecipitation results are

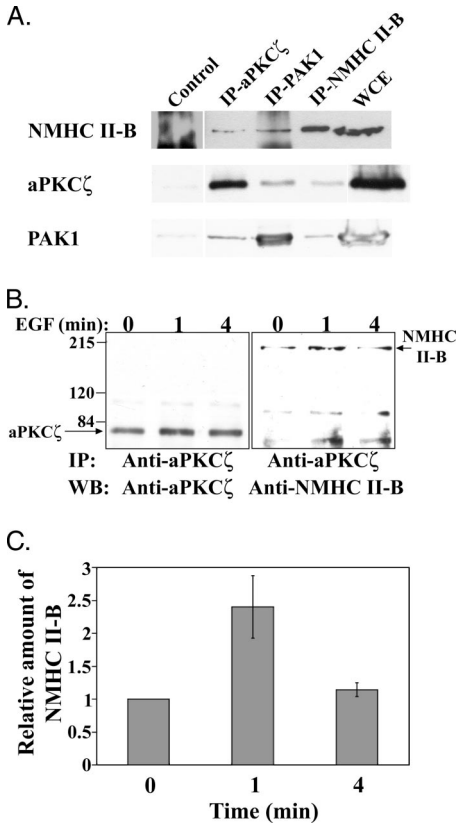

Figure 2. PAK1, aPKCζ, and NMHC II-B are all found in one complex and the interaction between aPKCζ and NMHC II-B is EGF-dependent. (A) Representative Western blots of coimmunoprecipitations of NMHC II-B, aPKCζ, and PAK1 from TSU-pr1 cells stimulated with EGF for 1 min. Immunoprecipitation was carried out using aPKCζ, PAK1, and NMHC II-B antibodies (IP-aPKCζ, IP-PAK1, and IP-NMHC II-B, respectively). Cdk7 antibodies or beads only were used as negative controls (Control). The immunoprecipitations were separated on SDS-PAGE, and Western blot was carried out using the antibodies indicated on the left. The amount of protein in the whole cell extract (WCE) represents ~50% of the total protein in the lysates used for the immunoprecipitation. (B) aPKCζ was immunoprecipitated from TSU-pr1 cell lysates that were stimulated with EGF for 0, 1, or 4 min and subjected to Western blot analysis using aPKCζ antibodies (left blot). The blot was then probed with anti-NMHC II-B antibody (right blot). Relative molecular masses (in thousands) are given to the left of the gels. The Western blot is representative of three experiments. (C) Quantification of three experiments as shown in B, presented as the amount of NMHC II-B that coimmunoprecipitates with aPKCζ at each time point after EGF stimulation, relative to the amount of NMHC II-B that coimmunoprecipitates with aPKCζ in unstimulated cells (mean ± SD). The amount of immunoprecipitated NMHC II-B at each time point was standardized by dividing its value with the value of the immunoprecipitated aPKCζ of that same time point.

consistent with results from immunofluorescent staining of NMHC II-B and aPKCζ in TSU-pr1 cells stimulated for the same time intervals with EGF (Figure 3).

The results described above indicate that NMHC II-B and aPKCζ interact. To study this possibility further, we investigated the cellular localization of aPKCζ and NMHC II-B. For this purpose we stimulated TSU-pr1 cells with EGF and subjected them to immunofluorescent staining using an antibody specific to aPKCζ and an antibody specific to NMHC II-B, as described in *Materials and Methods*. Without EGF stimulation NMHC II-B is mostly cytosolic (Figure 3A and see Straussman *et al.*, 2001), and aPKCζ is mostly located in the nucleus. After 1 min of EGF stimulation, most aPKCζ translocated to become mostly cytosolic with a small portion of the kinase located in the cell cortex. After 4 min of EGF stimulation, most of the aPKCζ had translocated back to the nucleus (Figure 3A). Concurrently, NMHC II-B was mostly located in the cell cortex 1 min after EGF stimulation and it remained there even after 4 min of EGF stimulation (Figure 3A). Analysis of several images such as those presented in Figure 3A indicated that after 1 min of EGF stimulation there was a significant increase in the number of cells that show areas of NMHC II-B and aPKCζ colocalization (~47%) compared with unstimulated cells (~19%) and cells that were stimulated with EGF for 4 min (~19%; Figure 3B). This colocalization after 1 min of EGF stimulation coincides with the peak of NMHC II-B coimmunoprecipitation with aPKCζ (Figure 2B). The results presented in Figures 2 and 3 indicate that the interaction of NMHC II-B and aPKCζ is EGF-dependent and that this interaction takes place mainly in the cell cortex.

Furthermore, our results indicate that aPKCζ's behavior in our cell system differs from other published studies (Bertolaso *et al.*, 1998; Neri *et al.*, 1999; Umar *et al.*, 2000). In these studies aPKCζ resides in the cytosol in unstimulated cells and enters the nucleus after stimulation (Bertolaso *et al.*, 1998; Neri *et al.*, 1999; Umar *et al.*, 2000), whereas in our system aPKCζ resides in the nucleus and exits to the cytosol and cell cortex after EGF stimulation. It should be noted that the cell lines and stimuli used in the various studies differ from each other and that the extent of stimulation in most studies was much longer than the few minutes that we applied in our studies.

aPKCζ Phosphorylates NMHC II-B Directly and Specifically

Our results have so far confirmed that NMHC II-B, PAK1, and aPKCζ form a complex in vivo and that the interaction between NMHC II-B and aPKCζ is EGF-dependent. Furthermore, the complex PAK1–aPKCζ, which is immunoprecipitated from cells, phosphorylates NMHC II-B in an EGF-dependent manner (Figure 1A and Even-Faitelson *et al.*, 2005). Although PAK1 and aPKCζ are involved in NMHC II-B phosphorylation, the data above reveals that PAK1 does not phosphorylate NMHC II-B directly (Figure 1B). The next step, therefore, was to explore the possibility that aPKCζ phosphorylates NMHC II-B. We first examined whether the aPKCζ immunoprecipitated from TSU-pr1 cells is capable of phosphorylating the NMHC II-B tail, with IP-PAK1 used for comparison. As shown in Figure 4A, IP-aPKCζ phosphorylated the NMHC II-B tail to the same extent as IP-PAK1. These results suggest that the myosin heavy chain kinase (MHCK) activity detected in IP-PAK1 represents aPKCζ activity.

To investigate whether aPKCζ phosphorylates NMHC II-B directly, we used recombinant aPKCζ to phosphorylate the NMHC II-B tail. We mixed recombinant aPKCζ with NMHC II-B tail fragment in the presence of ^{32}P-γATP. For a positive control, we used MHCK preparation from TSU-pr1 cells (Straussman *et al.*, 2001; Ben-Ya'acov and Ravid, 2003) to phosphorylate the NMHC II-B tail. As shown in Figure 4B, the recombinant aPKCζ directly phosphorylates the NMHC II-B tail. Furthermore, this phosphorylation is isoform specific because the recombinant aPKCζ did not phosphorylate NMHC II-A tail fragment (Figure 4B). These results are consistent with the findings that the IP-PAK1 complex phosphorylates NMHC II-B tail specifically, but does not phosphorylate NMHC II-A tail (Figure 1A and

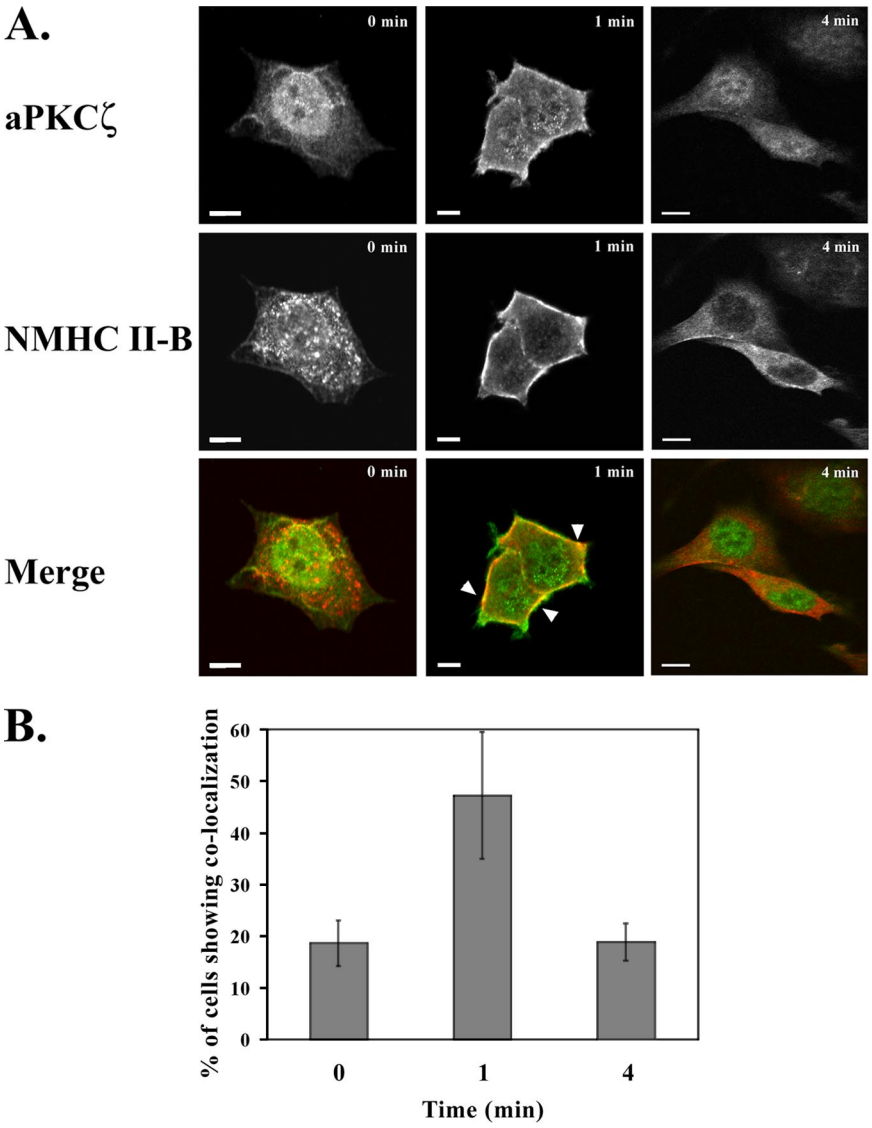

Figure 3. EGF-dependent localization of NMHC II-B and aPKCζ in TSU-pr1 cells. (A) Immunofluorescence staining of aPKCζ (top panels, green) and NMHC II-B (middle panels, red) in TSU-pr1 cells stimulated with EGF for 0, 1, or 4 min. Areas of colocalization are yellow and are indicated with arrowheads (Merge). Bar, 10 μm. (B) Quantification of the number of cells that exhibit colocalization between NMHC II-B and aPKCζ at each time point after EGF stimulation. The results are presented as mean ± SD of the percentage of cells that show colocalization out of the total number of random cells counted in three independent experiments (average total cells counted for each time point: n = 180).

Even-Faitelson *et al.*, 2005). Figure 4B also shows that MHCK preparation from TSU-pr1 cells phosphorylates NMHC II-B tail more extensively than recombinant aPKCζ. This is probably due to the fact that the MHCK preparation from TSU-pr1 cells contains other kinases that also phosphorylate NMHC II-B tail. We have shown that cPKC's are capable of phosphorylating NMHC II-B in TSU-pr1 cells (Straussman *et al.*, 2001). Additionally, we have recently found that cPKCγ also phosphorylates the NMHC II-B tail (Rosenberg and Ravid, 2006). Furthermore, the quantity of active aPKCζ in the MHCK preparation compared with the amount of active aPKCζ in the recombinant aPKCζ reaction is unknown.

Because in vitro phosphorylation of a small part of a molecule may be nonspecific, we wanted to confirm that aPKCζ is capable of phosphorylating the full-length NMHC II-B. To examine whether aPKCζ is capable of phosphorylating full-length NMHC II-B, we expressed GFP-NMHC II-B in COS-7 cells, immunoprecipitated the molecule using GFP antibodies, and subjected it to an in vitro phosphorylation assay using recombinant aPKCζ, as described above. As shown in Figure 4C, aPKCζ was able to phosphorylate the full-length NMHC II-B, as in the case of NMHC II-B tail. A negative control in which we performed the same phosphorylation reaction, but in the absence of recombinant aPKCζ, confirms that the phosphorylation of NMHC II-B was carried out by aPKCζ and not by an unknown enzyme that may have coimmunoprecipitated with the GFP-NMHC II-B. Furthermore, when GFP alone was expressed, immunoprecipitated, and subjected to the same phosphorylation assay, it was not phosphorylated by aPKCζ (Figure 4C), thereby confirming that the phosphorylation on GFP-NMHC II-B is on the NMHC II-B region of the fusion protein and not on the GFP.

aPKCζ Phosphorylates NMHC II-B In Vivo

Because in vitro phosphorylation assays may result in nonspecific phosphorylation of substrates, it was essential to study whether aPKCζ also phosphorylates NMHC II-B in vivo. For this purpose, we performed siRNA experiments in which the expression of aPKCζ in TSU-pr1 cells was decreased. These cells were labeled with ^{32}P-orthophosphate and the phosphorylation level of the endogenous NMHC II-B after 1 min of EGF stimulation was determined. The siRNA treatment led to an average decrease of ~50% in the protein level of aPKCζ (Figure 4D). As can be seen in Figure 4, E and F, the decrease in aPKCζ level led to a decrease of

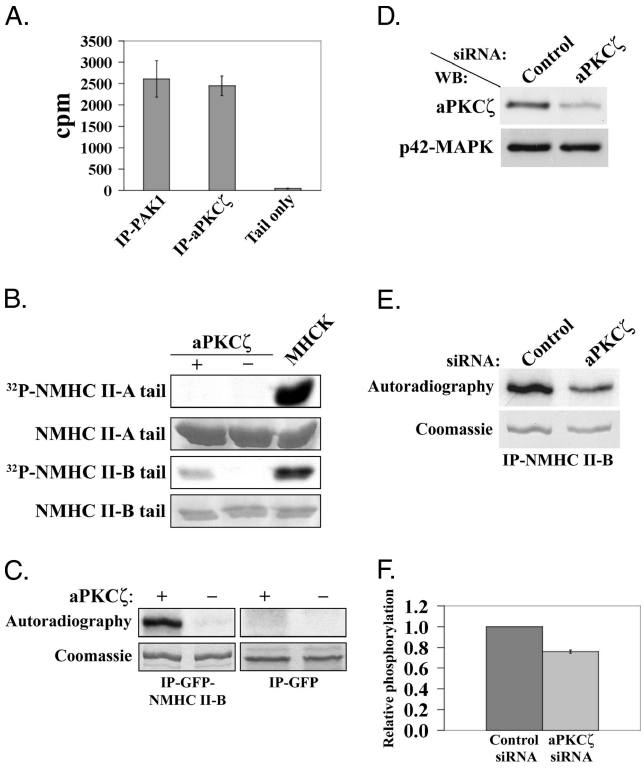

Figure 4. aPKCζ phosphorylates NMHC II-B directly in vitro and in vivo. (A) NMHC II-B tail phosphorylated by PAK1 or aPKCζ immunoprecipitated from TSU-pr1 cells (IP-PAK1 and IP-aPKCζ, respectively). As a negative control, the NMHC II-B tail was subjected to phosphorylation assay in the absence of IP-PAK1 or IP-aPKCζ (Tail only). The results are an average of two experiments ± SD. (B) NMHC II-A and NMHC II-B tail fragments were subjected to phosphorylation assay in the presence (+) or absence (−) of recombinant aPKCζ or MHCK preparation (Straussman *et al.*, 2001; Ben-Ya'acov and Ravid, 2003). The tail fragments were resolved on SDS-PAGE and stained with Coomassie brilliant blue followed by an autoradiogram. The results are representative of five experiments. (C) GFP-NMHC II-B full-length or GFP alone were expressed in COS-7 cells, immunoprecipitated using GFP antibodies and subjected to phosphorylation assay in the presence or absence of aPKCζ. The top panels show the phosphorylated proteins (IP-GFP-NMHC II-B or IP-GFP) detected by an autoradiogram (Autoradiography), and the bottom panels show the total proteins as seen in Coomassie blue staining (Coomassie). (D) A representative Western blot analysis of the aPKCζ protein level after transfection of TSU-pr1 cells with aPKCζ siRNA (aPKCζ) or control siRNA (Control). Cells were transfected with the siRNA 48 h before the experiment. Ten percent of the lysates were subjected to Western blot analysis using aPKCζ antibody followed by p42-MAPK antibody, as a loading control. (E) A representative in vivo phosphorylation experiment of NMHC II-B in cells treated with aPKCζ siRNA. NMHC II-B was immunoprecipitated from cell lysates transfected as described in D. The immunoprecipitates were separated on SDS-PAGE and then stained with Coomassie blue (Coomassie). The gel was scanned, dried, and exposed to film (Autoradiography). (F) A plot representing the amount of phosphorylated NMHC II-B in cells treated with aPKCζ siRNA relative to the amount of phosphorylated NMHC II-B in the control cells. The amount of phosphorylated NMHC II-B was calculated by dividing the value of the phosphorylated NMHC II-B band by the value of the total NMHC II-B band from the gel. The plot summarizes results of three experiments such as the one described in E.

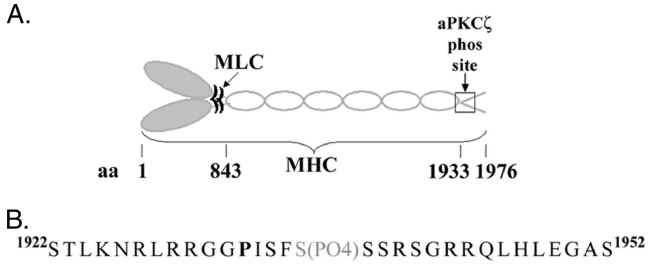

Figure 5. aPKCζ phosphorylates NMHC II-B tail on a serine residue on the nonhelical coiled coil C-terminus of myosin II-B. (A) Schematic representation of a myosin II-B molecule: a hexamer including two heavy chains and two pairs of light chains. The boxed area represents the region on the nonhelical tailpiece to which the aPKCζ phosphorylation site was mapped. (B) An enlargement of the boxed area in A, including the amino acid sequence surrounding the aPKCζ phosphorylation site. P (bold) represents the proline that breaks the α-helical coiled coil of the molecule. S (gray) represents the Ser[1937] residue, which is the aPKCζ phosphorylation site mapped by mass spectrometry.

~25% in NMHC II-B phosphorylation level in vivo. The relatively small decrease in the phosphorylation level of NMHC II-B may be due to the partial decrease in aPKCζ expression and the phosphorylation of NMHC II-B by other kinases. It is known that NMHC II-B is phosphorylated by kinases other than aPKCζ, such as CKII and cPKCγ (Murakami *et al.*, 1998; Rosenberg and Ravid, 2006). These kinases have ~10 potential phosphorylation sites and therefore it is likely that they contribute to the observed phosphorylation. It should be noted that the same experiments were also carried out in cells that were not stimulated with EGF, and in those cells we also observed a decrease in NMHC II-B phosphorylation, but to a lesser extent. This result may imply that aPKCζ is also involved in NMHC II-B basal phosphorylation.

aPKCζ Phosphorylates a Specific Serine Residue Located on the Nonhelically Coiled Coil Tail of Myosin II-B

Our results strongly suggest that aPKCζ phosphorylates NMHC II-B directly and in a specific manner. The next step was to map the specific amino acid(s) in the NMHC II-B tail that undergo(es) phosphorylation by aPKCζ. First, we determined the enzyme-substrate ratio (i.e., aPKCζ -NMHC II-B tail) giving maximal incorporation of phosphate into the substrate. To do this, we performed phosphorylation assays and calculated the amount of phosphate incorporated into the NMHC II-B tail (described in *Materials and Methods*). The optimal ratio was 1:6.8 moles (aPKCζ -NMHC II-B tail) and 1.48 ± 0.307 mol phosphates were incorporated per mol NMHC II-B tail. In a control experiment in which aPKCζ was omitted from the reaction mixture, the amount of phosphate incorporated into NMHC II-B was 0.007 ± 0.004 mol phosphate per mol NMHC II-B tail (for details see *Materials and Methods*). There are thus probably one or two sites of phosphorylation for aPKCζ on NMHC II-B tail.

To map the phosphorylation site, we performed mass spectrometry analysis on phosphorylated NMHC II-B tail in comparison to native NMHC II-B tail, as described in *Materials and Methods*. The phosphorylated peak was identified by comparing the spectra of the phosphorylated NMHC II-B tail to that of the native protein. MS/MS was performed on the dissimilar peaks of the two samples and then on the phosphorylated peak, which was identified at 615.8 M/z. The mass spectrometry analysis showed that aPKCζ phosphorylates the NMHC II-B tail on a serine residue at position 1937 (Ser[1937]) of the whole NMHC II-B protein (Figure 5A).

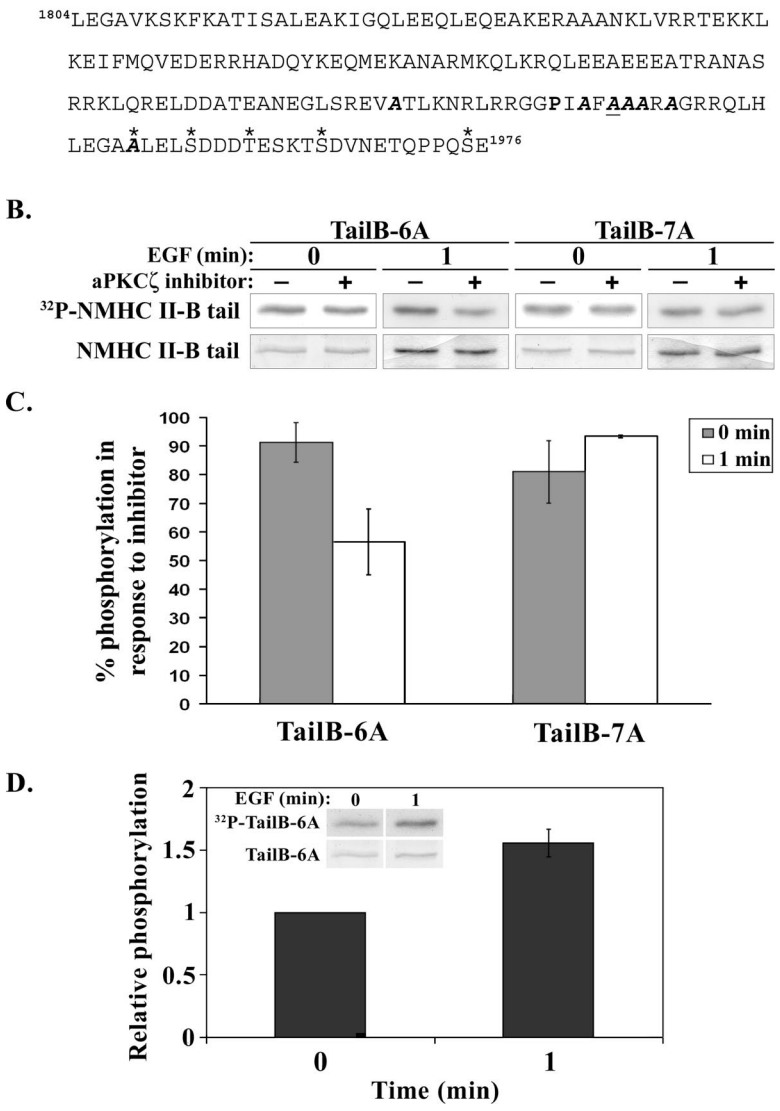

Figure 6. aPKCζ phosphorylates NMHC II-B on Ser[1937] in vivo in response to EGF stimulation. (A) Amino acid sequence of Tail-7A construct. P (bold) represents the proline that breaks the α-helical coiled coil of the molecule. A (bold italic) represent the PKC phosphorylation sites that were replaced with alanines. A (bold, italic, and underlined) represents the mapped aPKCζ phosphorylation site that was replaced with an alanine residue in the Tail-7A construct (this residue was not replaced in Tail-6A construct). Asterisk (*) marks the putative CKII phosphorylation sites (Murakami *et al.*, 1998). The bold italic A marked by an asterisk represents a serine residue replaced with alanine, which was mapped as a CKII phosphorylation site by Murakami *et al.* (1998) and as a PKC phosphorylation site by our lab (Rosenberg and Ravid, 2006). (B) In vivo phosphorylation of TailB-6A and TailB-7A. The fragments were expressed in TSU-pr1 cells, and their phosphorylation was examined in the presence or absence of a cell-permeable aPKCζ-specific inhibitor and with or without EGF stimulation. The bottom row shows the total protein, as seen in Coomassie staining; the row above that shows the phosphorylated proteins as seen in an autoradiogram. (C) The percent of Tail-6A and Tail-7A phosphorylation with or without EGF stimulation, after treatment with aPKCζ inhibitor. For each NMHC II-B fragment, the extent of phosphorylation in the presence of the inhibitor was compared with the extent of phosphorylation without inhibitor. The results are an average of three independent experiments ± SD. (D) The extent of phosphorylation of Tail-6A after 1 min after EGF stimulation relative to the extent of phosphorylation of Tail-6A from unstimulated cells. The graph represents the average relative phosphorylation of three separate experiments ± SD. The insets are a representative experiment, the top row shows the phosphorylated Tail-6A detected by an autoradiogram and the bottom row shows the total protein as seen in Coomassie staining.

This serine residue is located within a cluster of serine residues that reside in the nonhelical tailpiece (Figure 5B). This cluster of serine residues was previously suggested as a potential phosphorylation sites for PKC (Murakami *et al.*, 1998, 2000), but it should be pointed out that the PKC preparation used in Murakami *et al.*'s (1998, 2000) study was purified from rat brains and contained a mixture of kinases, mainly α, β, and γ isoforms of PKC.

aPKCζ Phosphorylates NMHC II-B In Vivo in Response to EGF Stimulation

Having found that aPKCζ phosphorylates NMHC II-B directly on a specific serine residue, we next investigated whether this phosphorylation also takes place in vivo and whether it is EGF-dependent. As mentioned above, there are several phosphorylation sites on the nonhelical tailpiece of NMHC II-B (Murakami *et al.*, 1998, 2000) and these may mask the change in phosphorylation of a single serine residue by aPKCζ. To avoid this difficulty, we expressed two C-terminal fragments of NMHC II-B in TSU-pr1 cells. In the first fragment the six serine residues that were mapped as potential PKC phosphorylation sites (Murakami *et al.*, 1998) were mutated to alanine, leaving the Ser[1937] intact (TailB-6A). The second fragment was mutated as described above, but the aPKCζ's phosphorylation site, Ser[1937], was also mutated to alanine (TailB-7A, Figure 6A). It is important to note that other phosphorylation sites, such as the casein kinase II (CKII) sites that also reside in the nonhelical tailpiece were left intact (Murakami *et al.*, 1998 and Figure 6A), thus allowing some phosphorylation on these fragments.

To examine the in vivo phosphorylation of TailB-6A and TailB-7A, we transiently transfected TSU-pr1 cells with plasmids encoding for the above fragments fused to GFP. We incubated these cells with ^{32}P-orthophosphate and then immunoprecipitated the fragments using specific NMHC II-B antibodies, as described in *Materials and Methods*. The in vivo phosphorylation of these fragments was examined in the presence or absence of a specific aPKCζ inhibitor and with or without 1 min of EGF stimulation (Figure 6B). As seen in Figure 6, B and C, aPKCζ inhibitor diminishes the phosphorylation level of TailB-6A in EGF-stimulated cells by ~45%,

with almost no affect on the phosphorylation level of TailB-7A in EGF-stimulated cells. Moreover, the phosphorylation level of the two fragments did not change significantly after treatment of unstimulated cells with aPKCζ inhibitor. It is important to note that the phosphorylation of TailB-6A increased in response to EGF stimulation (Figure 6D). These results are consistent with our previous studies showing that NMHC II-B is phosphorylated in response to EGF stimulation (Straussman *et al.*, 2001; Ben-Ya'acov and Ravid, 2003; Even-Faitelson *et al.*, 2005). These results indicate that aPKCζ phosphorylates NMHC II-B in vivo in response to 1-min EGF stimulation and that the phosphorylation takes place on Ser^{1937}, just as we mapped in vitro.

These results correlate with the results described in Figure 2B, which show that coimmunoprecipitation of NMHC II-B with aPKCζ is EGF-dependent and that the maximum amount of NMHC II-B that coimmunoprecipitates with aPKCζ is 1 min after EGF stimulation. Moreover, Figure 3 shows that only 1 min after EGF stimulation, when aPKCζ translocates from the nucleus to the cytoplasm, there are areas where NMHC II-B and aPKCζ colocalize. Taken together, these results suggest that 1 min after EGF stimulation, aPKCζ translocates from the nucleus to the cytoplasm and phosphorylates NMHC II-B on Ser^{1937}. The small decrease in the phosphorylation of the two fragments in the presence of the inhibitor in unstimulated cells (Figure 6C) may reflect an indirect involvement of aPKCζ in the basal phosphorylation of NMHC II-B on sites other than the mutated ones, such as the CKII sites, which were left intact.

A Mutation Mimicking Phosphorylation on an aPKCζ's Phosphorylation Site Leads to Slower Filament Assembly of Myosin II-B

Although it is well accepted that filament assembly of vertebrate nonmuscle myosin II is regulated by phosphorylation of the light chains, there is increasing evidence that phosphorylation of the C-terminal nonhelical tailpiece also plays a role in filament assembly (Tashiro *et al.*, 1985; Hodge *et al.*, 1992; Murakami *et al.*, 1995, 1998, 2000). Moreover, Murakami *et al.* (2000) have shown that assembly is affected by mutations mimicking phosphorylation on a serine cluster located on myosin II-B nonhelical tailpiece. However, none of these studies have shown whether assembly of myosin II-B is affected by phosphorylation on the single serine residue, which we mapped to be a phosphorylation site of aPKCζ on NMHC II-B. To address this issue, we first compared the critical concentration needed for filament assembly of an NMHC II-B fragment (NMHC II-B rod) in comparison with a mutant NMHC II-B rod in which the aPKCζ phosphorylation site was changed to aspartate (S1937D), as described in *Materials and Methods*. It should be noted that we recently found that the solubility characteristics of NMHC II-B rod are similar to those of the whole myosin II-B molecule (Straussman *et al.*, personal communication). We found that higher concentrations of protein are needed for the mutant S1937D rod to assemble into filaments. We tested this by dialyzing the proteins for 4 h against 150 mM NaCl and then centrifuging them at 100,000 × *g*. The wild-type NMHC II-B rod sediments almost entirely at a concentration of 15 and 25 μg/ml (only ~6% of the protein is soluble), but a considerable amount of the S1937D rod was soluble at 15 or 25 μg/ml (~39% or ~31%, respectively). These results indicate that the S1937D mutation does change the assembly properties of the NMHC II-B rod.

We next determined whether the S1937D mutation changes the assembly kinetics of NMHC II-B rod. We again dialyzed the proteins against 150 mM NaCl, but this time we took out samples 1, 1.5, 2, 3, and 4 h after dialysis (as described in *Materials and Methods*). At these time points the osmolarity of the protein samples had reached the osmolarity of the dialysis solution (unpublished data). We next centrifuged the samples at 100,000 × *g* and separated the supernatant, containing soluble NMHC II-B rod, from the pellet, containing NMHC II-B rod that had assembled into filaments (Figure 7A).

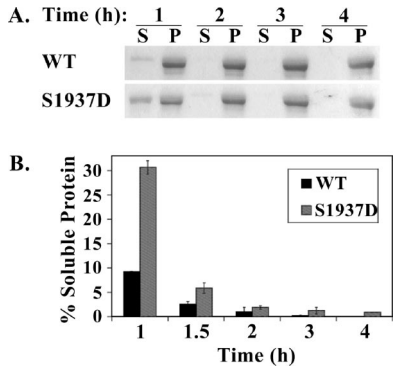

Figure 7. A mutation mimicking phosphorylation on the aPKCζ phosphorylation site leads to slower filament assembly. (A) A representative Coomassie-stained SDS-PAGE of a solubility assay of NMHC II-B rod wild type (WT) and mutant, in which the aPKCζ phosphorylation site was changed to aspartate (S1937D). The proteins were dialyzed in 150 mM NaCl buffer for 1, 2, 3, or 4 h, and after centrifugation the supernatant (soluble NMHC II-B rod) and pellet (filamentous NMHC II-B rod) were separated on SDS-PAGE. (B) A plot of the relative amount of soluble NMHC II-B rod WT or S1937D mutant after 1, 1.5, 2, 3, and 4 h of dialysis in 150 mM NaCl buffer. Relative amount of soluble protein was calculated by dividing the amount of protein in the supernatant by the sum of the total protein in the supernatant and pellet fractions. The graph represents results from three independent experiments such as those described in A.

After 1 h of dialysis, ~10% of the wild-type NMHC II-B rod was soluble, in contrast to ~30% of the S1937D mutant (Figure 7B). After 1.5 h of dialysis only ~3% of the wild-type NMHC II-B rod, but ~7% of the S1937D mutant, was soluble (Figure 7B). After 2, 3, and 4 h of dialysis the two proteins showed similar solubility properties, and both were found in the nonsoluble fraction, indicating that both had assembled into filaments (Figure 7). These results suggest that a mutation mimicking phosphorylation on the aPKCζ phosphorylation site leads to slower filament assembly of myosin II-B.

These results show that a single mutation mimicking phosphorylation on Ser^{1937} on NMHC II-B, which is the phosphorylation site of aPKCζ, alters the filament assembly properties of myosin II-B. The S1937D mutation increases the critical concentration of the protein and slows down filament assembly. On the whole, these results imply that phosphorylation of aPKCζ on myosin II-B disrupts filament assembly.

PAK1 Is Involved in the Phosphorylation of aPKCζ

As PAK1 and aPKCζ reside in one complex, PAK1 may be able to phosphorylate aPKCζ directly. To test whether this is indeed the case, we expressed $aPKC\zeta^{WT}$ fused to hemagglutinin (HA) in HEK-293 cells and then immunoprecipitated it with anti-HA antibodies as described in *Materials and Methods*. We subjected the immunoprecipitate to in vitro kinase assay in the presence or absence of recombinant GST-PAK1. As shown in Figure 8, $aPKC\zeta^{WT}$ is phosphorylated to a much greater extent in the presence of GST-PAK1. The weak

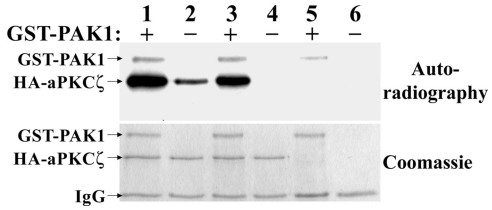

Figure 8. PAK1 can phosphorylate aPKCζ in vitro. HA-aPKCζ wild-type (lanes 1 and 2), HA-aPKCζ kinase dead (lanes 3 and 4), or a GFP control (lanes 5 and 6) were transfected to HEK-293 cells and immunoprecipitated. The immunoprecipitate was subjected to an in vitro kinase assay in the presence (lanes 1, 3, and 5) or absence (lanes 2, 4, and 6) of recombinant GST-PAK1. The proteins were then separated on SDS-PAGE, stained with Coomassie brilliant blue (bottom panel), and exposed to autoradiography (top panel). The results are representative of three separate experiments.

phosphorylation of aPKCζ^{WT} seen in the absence of GST-PAK1 can probably be accounted for by the autophosphorylation undergone by many PKCs (Newton and Koshland, 1987; Newton, 1997; Ron and Kazanietz, 1999). To check this, we expressed a kinase-dead mutant of aPKCζ (aPKCζ^{KD}) and subjected it to the same kinase assay. As shown in Figure 8, aPKCζ^{KD} was phosphorylated only in the presence of GST-PAK1, indicating that the phosphorylation seen on aPKCζ^{WT} in the absence of GST-PAK1 is indeed due to autophosphorylation and that GST-PAK1 phosphorylates aPKCζ directly.

The above results indicate that PAK1 phosphorylates aPKCζ in vitro. To test whether PAK1 phosphorylates aPKCζ also in vivo, we performed in vivo phosphorylation experiments of aPKCζ in TSU-pr1 cells transfected with PAK1 versus control siRNA. TSU-pr1 cells were transfected with PAK1 or fluorescein-conjugated control siRNA. To assess transfection efficiency of the control cells, 48 h after the transfection the cells were observed using a fluorescence microscope and then an in vivo phosphorylation assay was carried out, as described in *Materials and Methods.* The efficiency of PAK1 siRNA was assessed by separating treated cells lysate on 10% SDS-PAGE followed by Western blot analysis using PAK1 antibody and p42-MAPK antibody, for loading control. To measure the extent of phosphorylation of aPKCζ in vivo in PAK1 siRNA-treated cells and control siRNA-treated cells, the immunoprecipitated aPKCζ was separated on SDS-PAGE, the gel was stained and then exposed to film. The fluorescence of the cells transfected with control siRNA revealed ~98% transfection efficiency, indicating that the cells were well transfected. As shown in Figure 9A, transfection of cells with PAK1 siRNA decreased the PAK1 protein expression level to 20–45% of that of cells transfected with the control siRNA.

Figure 9C clearly shows that aPKCζ phosphorylation is decreased by ~50% in cells transfected with PAK1 siRNA compared with cells transfected with control siRNA. Thus implicating that the decrease in PAK1 protein level leads to decrease in aPKCζ phosphorylation. Evidently, these results demonstrate that PAK1 is involved in aPKCζ phosphorylation in vivo and therefore supports the in vitro results that show that recombinant PAK1 phosphorylates aPKCζ. It should be noted that experiments were carried out in cells that were not stimulated with EGF, indicating that PAK1's involvement in aPKCζ phosphorylation is not EGF-dependent. When the same experiments was carried out with cells that were stimulated for 1 min with EGF, a decrease in aPKCζ phosphorylation level was observed, as well, but this

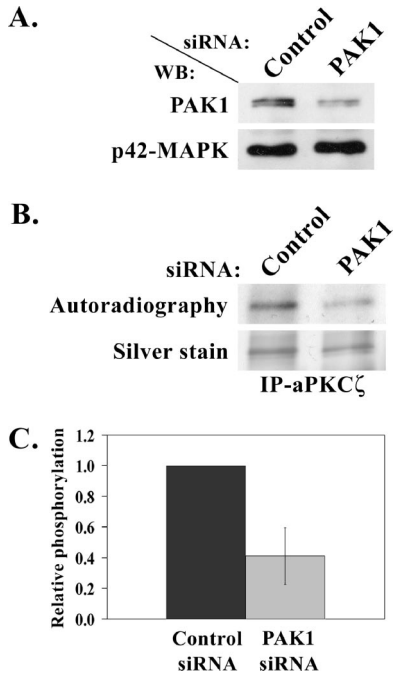

Figure 9. PAK1 is involved in aPKCζ phosphorylation in vivo. (A) A representative Western blot showing PAK1 protein level after transfection of TSU-pr1 cells with PAK1 siRNA (PAK1) or fluorescein-conjugated control siRNA (Control). Cells were transfected with the siRNA 48 h before the experiment. To determine the expression level of PAK1 in siRNA cells, 10% of the lysates were subjected to Western blot analysis using PAK1 antibody followed by p42-MAPK antibody, as a loading control. (B) A representative in vivo phosphorylation experiment of aPKCζ. aPKCζ was immunoprecipitated from cell lysates transfected as described in A. The immunoprecipitates were separated on SDS-PAGE, which was then stained with silver stain. The gel was scanned, dried, and exposed to film (Autoradiography). (C) A plot representing the amount of phosphorylated aPKCζ in cells treated with PAK1 siRNA relative to the amount of phosphorylated aPKCζ in the control cells. The amount of phosphorylated aPKCζ was calculated by dividing the value of the phosphorylated aPKCζ band by the value of the total aPKCζ band from the gel. The plot summarizes results of three experiments such as the one described in B.

decrease was statistically insignificant (unpublished data). These results may indicate that upon EGF stimulation kinases other than PAK1 also phosphorylate aPKCζ (Newton, 1997).

A Decrease in aPKCζ's Expression Alters NMHC II-B Cellular Organization

We next wanted to see whether aPKCζ indeed plays a role in NMHC II-B regulation after EGF stimulation in vivo. To study the effect of aPKCζ on the cellular localization and organization of NMHC II-B upon EGF stimulation, we reduced the expression of aPKCζ in the cells using siRNA. These cells were stimulated with EGF for 1 min and subjected to indirect immunofluorescent staining using specific antibodies directed against aPKCζ and NMHC II-B as described in *Materials and Methods.* The micrographs in Figure 10A clearly demonstrate that lower levels of aPKCζ expression in the cells correlate with diffused appearance of NMHC II-B localization in those cells. It is also noticeable that in the same field of cells that were treated with aPKCζ siRNA there are also cells that show a higher level of expression of aPKCζ

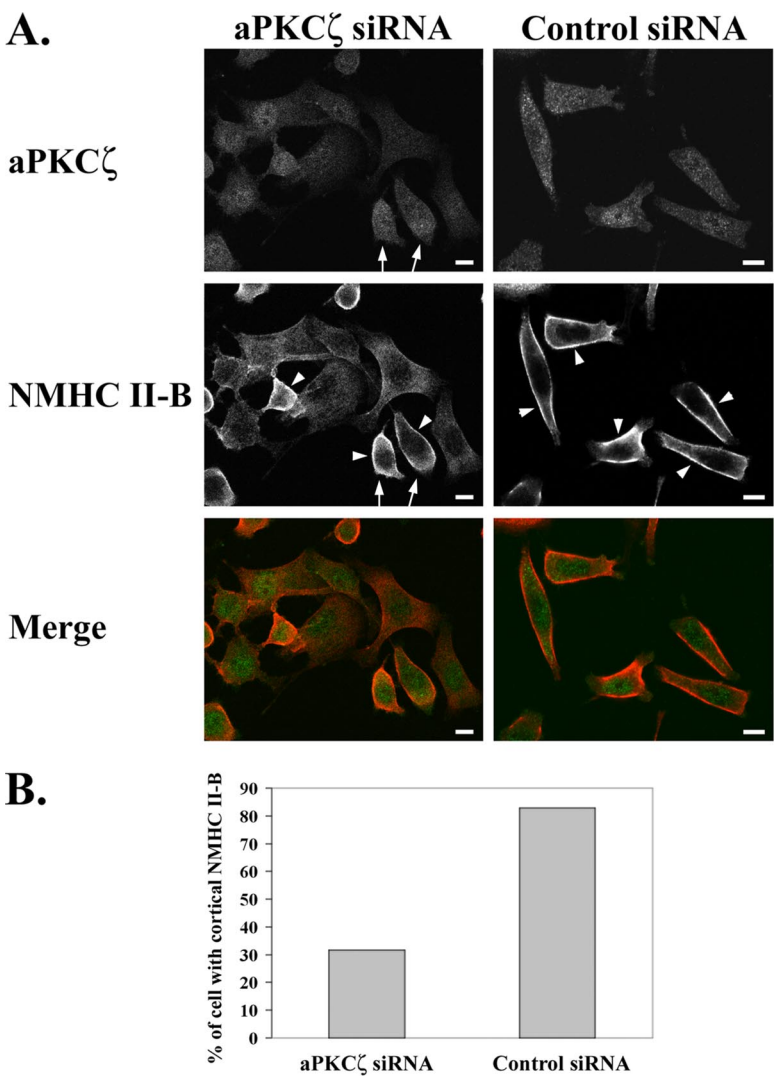

Figure 10. Reduced aPKCζ expression alters EGF-dependent NMHC II-B cellular localization and organization. (A) immunofluorescence staining of aPKCζ (top panels, green) and NMHC II-B (middle panels, red) in TSU-pr1 cells transfected with either aPKCζ siRNA (left panels) or control siRNA (right panels) and stimulated with EGF for 1 min. Arrows point to cells that show relatively high levels of aPKCζ expression in the aPKCζ siRNA cell population. Arrowheads point to cortical localization of NMHC II-B. Bar, 10 μm. (B) Quantification of the number of cells that exhibit cortical localization of NMHC II-B in cells transfected with aPKCζ siRNA compared with control siRNA. The results are presented as the percentage of cells that show cortical localization out of the total number of cells counted in 10 random fields (average total of cells counted for each type of siRNA treatment: n = 200).

(Figure 10A, arrows), and in those cells, that serve as an internal control, it is clear that NMHC II-B localizes to the cell cortex (Figure 10A, arrowheads). The existence of cells expressing higher levels of aPKCζ in the siRNA-treated cells is expected because, as was mentioned above, the decrease in the total expression of aPKCζ after siRNA treatment is only ~50%. Furthermore, it is clear from Figure 10, A and B, that transfection with aPKCζ siRNA leads to fewer cells that show NMHC II-B cortical localization after EGF stimulation, compared with transfection with control siRNA (32 vs. 83%, respectively). The results presented here clearly indicate that a decrease in aPKCζ expression alters the localization and organization of NMHC II-B after EGF stimulation, causing it to be more diffused and not localize to the cell cortex.

DISCUSSION

Signal transduction in cells is one of the most intensely researched fields in biology today. Many signaling pathways in mammalian cells involve different signaling proteins that lead to different processes, but the number of signaling proteins does not correlate with the enormous number of diverse processes that these proteins regulate. A plausible explanation for the particular role of a signaling protein in response to a specific signal at a specific cellular localization is the existence of anchoring proteins that enable the formation of specific signaling complexes (Pawson and Scott, 1997). These protein complexes may include a number of signaling proteins as well as the substrate to be regulated.

Our results define a novel signal transduction pathway that is regulated by EGF and includes PAK1 and aPKCζ as signaling proteins involved in the regulation of NMHC II-B phosphorylation and cellular organization. Indeed, we have shown a specific interaction between PAK1, aPKCζ, and NMHC II-B. Comparing the quantity of NMHC II-B that coimmunoprecipitates with PAK1 and aPKCζ with the total cellular NMHC II-B, represented in the whole cell extract shown in Figure 2A, implies that only a relatively small quantity of the total cellular NMHC II-B coimmunoprecipitates with PAK1 and aPKCζ (Figure 2A). This may be due to the existence of specific signaling complexes that include PAK1, aPKCζ, and NMHC II-B and are localized at specific cellular sites for specific functions. The findings that PAK1 and aPKCζ specifically regulate the phosphorylation of NMHC II-B, but not NMHC II-A, supports the previous suggestions that these two isoforms are regulated differently and play different roles in the cell (Murakami *et al.*, 2000).

We mapped Ser^{1937} to be aPKCζ's phosphorylation site on NMHC II-B and have shown that aPKCζ phosphorylates NMHC II-B both in vitro and in vivo. Mimicking phosphorylation at this site leads to slower filament formation of NMHC II-B. Moreover, we have shown previously that expression of PAK1 mutants (constitutively active and dominant negative) alters the assembly properties of NMHC II-B in TSU-pr1 cells (Even-Faitelson *et al.*, 2005). Together, these results indicate that aPKCζ phosphorylation on Ser^{1937} plays a role in the regulation of myosin II-B filament assembly at certain sites in the cell. Furthermore, the colocalization of NMHC II-B and aPKCζ in the cell cortex in response to EGF stimulation (Figure 3) indicates that aPKCζ regulates NMHC II-B in a specific compartment of the cell in an EGF-dependent manner. To our knowledge this is the first study showing that PAK1 is involved in aPKCζ phosphorylation in vivo and is capable of phosphorylating aPKCζ directly in vitro. It appears that the involvement of PAK1 in aPKCζ phosphorylation occurs in cells that are not stimulated with EGF, meaning that although the interaction between aPKCζ and NMHC II-B seems to be EGF-dependent, the interaction between PAK1 and aPKCζ may not be EGF-dependent.

We believe that our results showing that PAK1 phosphorylates aPKCζ and that aPKCζ phosphorylates NMHC II-B in vivo, along with the findings that the interaction and phosphorylation of NMHC II-B by aPKCζ is EGF-dependent, support the physiological relevance of this signaling cascade. On the basis of the results presented here, we propose a model by which EGF stimulation of cells leads to reorganization of myosin II-B. PAK1 is involved in aPKCζ phosphorylation, but this function appears not to be dependent on EGF, because siRNA of PAK1 decreases aPKCζ phosphorylation in unstimulated cells (Figure 9). After EGF stimulation, aPKCζ translocates from the nucleus to the cytoplasm (Figure 3) and is therefore able to interact with myosin II-B. aPKCζ phosphorylates NMHC II-B on Ser^{1937}, which is located on the nonhelical tailpiece, leading to filament disassembly at certain sites of the cell. Results from our laboratory, as well as from others, indicate that other kinases, among them PKC isoforms, phosphorylate several sites on NMHC II-B, and this phosphorylation also affects filament assembly (Murakami *et al.*, 1998, 2000; Rosenberg and Ravid, 2006). It is therefore plausible that the early phosphorylation of NMHC II-B by aPKCζ after EGF stimulation (only 1 min after stimulation) destabilizes the myosin II-B filaments and primes other phosphorylation events carried out by other kinases. This later phosphorylation leads to maximal phosphorylation of NMHC II-B at ~6 min after EGF stimulation (Straussman *et al.*, 2001; Ben-Ya'acov and Ravid, 2003) and concomitantly to further filament disassembly.

Moreover, we also show that reduction in aPKCζ expression in the cells after siRNA treatment leads to altered NMHC II-B organization and cortical localization after EGF stimulation, causing NMHC II-B to appear more diffused and less localized to the cortex (Figure 10). This phenotype suggests that a reduction in aPKCζ expression impairs the ability of NMHC II-B to assemble into filaments in the cell cortex after EGF stimulation. This may be due to the lack of phosphorylation by aPKCζ, which is important for the disassembly of myosin II-B filaments in specific cellular sites, allowing filament assembly at new sites, such as the cell cortex. Many of the cells that show reduced expression of aPKCζ after siRNA treatment also have a more flattened appearance and are less polarized (Figure 10A). This could be explained by the involvement of NMHC II-B in a number of cytoskeletal structures, such as focal adhesions (Ben-Ya'acov and Ravid, 2003). It should be noted that the strong phenotype observed in the aPKCζ siRNA-treated cells may also partially be accounted for by the involvement of aPKCζ in the regulation of other cytoskeletal proteins, such as actin (Gomez *et al.*, 1995, 1997; Laudanna *et al.*, 1998; Uberall *et al.*, 1999; Hellbert *et al.*, 2000; Chodniewicz and Zhelev, 2003).

Together, the above results suggest that aPKCζ is an important NMHC II-B kinase, in general, which also plays a more specific role in the signaling cascade downstream to PAK1. Moreover, the results presented in Figure 10 support the theory that aPKCζ serves as a "priming kinase." Reducing the expression of aPKCζ has a dramatic effect on NMHC II-B EGF-dependent localization, beyond what one would expect from a kinase that can phosphorylates only one or two sites (there are a total of ~10 sites mapped as PKC and CKII phosphorylation sites on the NMHC II-B tailpiece). These results may indicate that reducing the expression of aPKCζ leads to a decrease in the amount of NMHC II-B that can be phosphorylated by PKC and/or CKII, thus preventing its reorganization and localization to the cell cortex.

Myosin II is a crucial and integral part of the cellular cytoskeleton and, as such, it plays an important role in many dynamic cellular processes, such as adhesion and motility. Myosin II plays diverse roles at different cellular sites in response to different cellular signals, probably through the formation of specific signaling complexes that regulate myosin II in certain cellular compartments in response to specific stimuli. The dynamic nature of the cellular processes in which myosin II is involved requires specific and localized regulation of the assembly properties of this protein. The type of isoform specific regulation at certain cellular sites introduced in this study suggests a mechanism for carrying out the complex dynamic cytoskeletal reorganization necessary in response to growth factor stimulation.

ACKNOWLEDGMENTS

We thank Daniel Ronen and Michael Rosenberg for their excellent technical assistance with the confocal laser microscopy experiments and Dr. Ofra Moshel for technical assistance with the mass spectrometry. We also thank Dr. Robert S. Adelstein, Laboratory of Molecular Cardiology NIH/NHLBI, Bethesda, MD, for NMHC II-B N-terminal antibodies; Dr. Gary M. Bokoch, Department of Immunology, The Scripps Research Institute, CA, for the recombinant GST-PAK1; and Dr. Yehiel Zick, Department of Molecular Cell Biology, The Weizmann Institute of Science, for the pCDNA3-HA-aPKCζ$^{WT/KD}$. We also thank all the members of S. Ravid's laboratory for their excellent and productive ideas. The work was supported by grants from Israel Academy for Sciences and Humanities, Israel Cancer Research Foundation, Israel Ministry of Health, and Israel Cancer Association.

REFERENCES

Ben-Ya'acov, A., and Ravid, S. (2003). Epidermal growth factor-mediated transient phosphorylation and membrane localization of myosin II-B are required for efficient chemotaxis. J. Biol. Chem. *278*, 40032–40040.

Berg, J. S., Powell, B. C., and Cheney, R. E. (2001). A millennial myosin census. Mol. Biol. Cell *12*, 780–794.

Bertolaso, L., Gibellini, D., Secchiero, P., Previati, M., Falgione, D., Visani, G., Rizzoli, R., Capitani, S., and Zauli, G. (1998). Accumulation of catalytically active PKC-zeta into the nucleus of HL-60 cell line plays a key role in the induction of granulocytic differentiation mediated by all-trans retinoic acid. Br. J. Haematol. *100*, 541–549.

Burgess, R. R. (1991). Use of polyethyleneimine in purification of DNA-binding proteins. Methods Enzymol. *208*, 3–10.

Buxton, D. B., Golomb, E., and Adelstein, R. S. (2003). Induction of nonmuscle myosin heavy chain II-C by butyrate in RAW 264.7 mouse macrophages. J. Biol. Chem. *278*, 15449–15455.

Chen, C., and Okayama, H. (1987). High-efficiency transformation of mammalian cells by plasmid DNA. Mol. Cell. Biol. *7*, 2745–2752.

Cheng, T.P.O., Murakami, N., and Elzinga, M. (1992). Localization of myosin-IIB at the leading edge of growth cones from rat dorsal-root ganglionic cells. FEBS Lett. *311*, 91–94.

Chodniewicz, D., and Zhelev, D. V. (2003). Chemoattractant receptor-stimulated F-actin polymerization in the human neutrophil is signaled by 2 distinct pathways. Blood *101*, 1181–1184.

Conti, M. A., Sellers, J. R., Adelstein, R. S., and Elzinga, M. (1991). Identification of the serine residue phosphorylated by PKC in vertebrate nonmuscle myosin heavy chains. Biochemistry *30*, 966–970.

Dulyaninova, N. G., Malashkevich, V. N., Almo, S. C., and Bresnick, A. R. (2005). Regulation of myosin-IIA assembly and Mts1 binding by heavy chain phosphorylation. Biochemistry *44*, 6867–6876.

Etienne-Manneville, S., and Hall, A. (2003). Cdc42 regulates GSK-3beta and adenomatous polyposis coli to control cell polarity. Nature *421*, 753–756.

Even-Faitelson, L., Rosenberg, M., and Ravid, S. (2005). PAK1 regulates myosin II-B phosphorylation, filament assembly, localization and cell chemotaxis. Cell Signal *17*, 1137–1148.

Gomez, J., Garcia, A., R.-Borlado, L., Bonay, P., Martinez-A., C., Silva, A., Fresno, M., Carrera, A. C., Eicher-Streiber, C., and Rebollo, A. (1997). IL-2 signaling controls actin organization through Rho-like protein family, phosphatidylinositol 3-kinase, and PKC-zeta. J. Immunol. *158*, 1516–1522.

Gomez, J., Martinez de Aragon, A., Bonay, P., Pitton, C., Garcia, A., Silva, A., Fresno, M., Alvarez, F., and Rebollo, A. (1995). Physical association and functional relationship between PKC zeta and the actin cytoskeleton. Eur. J. Immunol. *25*, 2673–2678.

Hellbert, K., Kampfer, S., Maly, K., Hochholdinger, F., Mwanjewe, J., Baier, G., Uberall, F., and Grunicke, H. H. (2000). Implication of atypical PKC isozymes lambda and zeta in Ras mediated reorganization of the actin cytoskeleton and cyclin D1-induction. Adv. Enzyme Regul. *40*, 49–62.

Hodge, T. P., Cross, R., and Kendrick-Jones, J. (1992). Role of the COOH-terminal nonhelical tailpiece in the assembly of a vertebrate nonmuscle myosin rod. J. Cell Biol. *118*, 1085–1095.

Iizumi, T., Yazaki, T., Kanoh, S., Kondo, I., and Koiso, K. (1987). Establishment of a new prostatic carcinoma cell line (TSU-pr1). J. Urol. *137*, 1304–1306.

Ikebe, M., Hartshorne, D. J., and Elzinga, M. (1987). Phosphorylation of the 20,000-dalton light chain of smooth muscle myosin by the calcium-activated, phospholipid-dependent protein kinase. Phosphorylation sites and effects of phosphorylation. J. Biol. Chem. *262*, 9569–9573.

Ikebe, M., Inagaki, M., Kanamaru, K., and Hidaka, H. (1985). Phosphorylation of smooth muscle myosin light chain kinase by Ca2+-activated, phospholipid-dependent protein kinase. J. Biol. Chem. *260*, 4547–4550.

Jaffer, Z., and Chernoff, J. (2002). p21-activated kinases: three more join the Pak. Int. J. Biochem. Cell Biol. *34*, 713–717.

Katsuragawa, Y., Yanagisawa, M., Inoue, A., and Masaki, T. (1989). Two distinct nonmuscle myosin heavy chain mRNAs are differently expressed in various chicken tissues. Eur. J. Biochem. *184*, 611–616.

Kawamoto, S., and Adelstein, R. S. (1991). Chicken nonmuscle myosin heavy chains: differential expression of two mRNAs and evidence for two different polypeptides. J. Cell Biol. *112*, 915–924.

Keenan, C., and Kelleher, D. (1998). PKC and the cytoskeleton. Cell Signal, *10*, 225–232.

Kelley, C. A., Sellers, J. R., Gard, D. L., Bui, D., Adelstein, R. S., and Baines, I. C. (1996). *Xenopus* nonmuscle myosin heavy chain isoforms have different subcellular localizations and enzymatic activities. J. Cell Biol. *134*, 675–687.

Knaus, U. G., and Bokoch, G. M. (1998). The p21Rac/Cdc42-activated kinases (PAKs). Int. J. Biochem. Cell Biol. *30*, 857–862.

Laudanna, C., Mochly-Rosen, D., Liron, T., Constantin, G., and Butcher, E. C. (1998). Evidence of zeta PKC involvement in polymorphonuclear neutrophil integrin-dependent adhesion and chemotaxis. J. Biol. Chem. *273*, 30306–30315.

Maupin, P., Phillips, C. L., Adelstein, R. S., and Pollard, T. D. (1994). Differential localization of myosin-II isozymes in human cultured cells and blood cells. J. Cell Sci. *107*, 3077–3090.

McNally, E., Sohn, R., Frankel, S., and Leinwand, L. (1991). Expression of myosin and actin in *Escherichia coli*. Methods Enzymol. *196*, 368–389.

Miller, M., Bower, E., Levitt, P., Li, D., and Chantler, P. D. (1992). Myosin II distribution in neurons is consistent with a role in growth cone motility but not synaptic vesicle mobilization. Neuron *8*, 25–44.

Murakami, N., Chauhan, V.P.S., and Elzinga, M. (1998). Two nonmuscle myosin II heavy chain isoforms expressed in rabbit brains: filaments forming properties, the effects of phosphorylation by PKC and casein kinase II, and location of the phosphorylation sites. Biochemistry *37*, 1989–2003.

Murakami, N., Elzinga, M., Singh, S. S., and Chauhan, V. P. (1994). Direct binding of myosin II to phospholipid vesicles via tail regions and phosphorylation of the heavy chains by PKC. J. Biol. Chem. *269*, 16082–16090.

Murakami, N., Kotula, L., and Hwang, Y.-W. (2000). Two distinct mechanisms for regulation of nonmuscle myosin assembly via the heavy chain: phosphorylation for MIIB and Mts 1 binding for MIIA. Biochemistry *39*, 11441–11451.

Murakami, N., Singh, S. S., Chauhan, V.P.S., and Elzinga, M. (1995). Phospholipid binding, phosphorylation by PKC, and filament assembly of the COOH terminal heavy chain fragments of nonmuscle myosin II isoforms MIIA and MIIB. Biochemistry *34*, 16046–16055.

Neri, L. M., Martelli, A. M., Borgatti, P., Colamussi, M. L., Marchisio, M., and Capitani, S. (1999). Increase in nuclear phosphatidylinositol 3-kinase activity and phosphatidylinositol (3,4,5) trisphosphate synthesis precede PKC-zeta translocation to the nucleus of NGF-treated PC12 cells. FASEB J. *13*, 2299–2310.

Newton, A. C. (1997). Regulation of PKC. Curr. Opin. Cell Biol. *9*, 161–167.

Newton, A. C., and Koshland, D.E.J. (1987). PKC autophosphorylation by an intrapeptide reaction. J. Biol. Chem. *262*, 10185–10188.

Pandey, A., Andersen, J. S., and Mann, M. (2000). Use of mass spectrometry to study signaling pathways. Sci. STKE *2000*, PL1.

Pawson, T., and Scott, J. D. (1997). Signaling through scaffold, anchoring, and adaptor proteins. Science *278*, 2075–2080.

Rochlin, M. W., Itoh, K., Adelstein, R. S., and Bridgman, P. C. (1995). Localization of myosin IIA and B isoforms in cultured neurons. J. Cell Sci. *108*, 3661–3670.

Ron, D., and Kazanietz, M. G. (1999). New insights into the regulation of PKC and novel phorbol ester receptors. FASEB J. *13*, 1658–1676.

Rosenberg, M., and Ravid, S. (2006). Protein kinase Cγ regulates myosin IIB phosphorylation, cellular localization, and filament assembly. Mol. Biol. Cell *17*, 1364–1374.

Simanis, V., and Lane, D. (1985). An immunoaffinity purification procedure for SV40 large T antigen. Virology *144*, 88–100.

Straussman, R., Even, L., and Ravid, S. (2001). Myosin II heavy chain isoforms are phosphorylated in an EGF-dependent manner: involvement of PKC. J. Cell Sci. *114*, 3047–3057.

Su, Z., and Kiehart, D. (2001). PKC phosphorylates nonmuscle myosin-II heavy chain from *Drosophila* but regulation of myosin function by this enzyme is not required for viability in flies. Biochemistry *40*, 3606–3614.

Tashiro, Y., Kumon, A., Yasuda, S., Murakami, N., and Matsumura, S. (1985). Two chymotrypsin-susceptible sites of myosin rod from chicken gizzard. Eur. J. Biochem. *148*, 521–528.

Turbedsky, K., Pollard, T. D., and Bresnick, A. R. (1997). A subset of PKC phosphorylation sites on the myosin II regulatory light chain inhibits phosphorylation by myosin light chain kinase. Biochemistry *36*, 2063–2067.

Uberall, F., Hellbert, K., Kampfer, S., Maly, K., Villunger, A., Spitaler, M., Mwanjewe, J., Baier-Bitterlich, G., Baier, G., and Grunicke, H. H. (1999). Evidence that atypical PKC-lambda and atypical PKC-zeta participate in Ras-mediated reorganization of the F-actin cytoskeleton. J. Cell Biol. *144*, 413–425.

Umar, S., Sellin, J. H., and Morris, A. P. (2000). Increased nuclear translocation of catalytically active PKC-zeta during mouse colonocyte hyperproliferation. Am. J. Physiol. Gastrointest. Liver Physiol. *279*, G223–G237.

van Leeuwen, F. N., van Delft, S., Kain, H. E., van der Kammen, R. A., and Collard, J. G. (1999). Rac regulates phosphorylation of the myosin II-heavy chain, actomyosin disassembly and cell spreading. Nat. Cell Biol. *1*, 242–248.